The Encapsulation of Ferrocyanide by Copper(II) Complexes of Tripodal Tetradentate Ligands. Novel H-Bonding Networks Incorporating Heptanuclear and Pentanuclear Heterometallic Assemblies

Richard J. Parker,[†] Leone Spiccia,*[,†] Stuart R. Batten,[†] John D. Cashion,[‡] and Gary D. Fallon[†]

School of Chemistry, PO Box 23, Monash University, Victoria 3800, Australia, and Department of Physics, PO Box 27, Monash University, Victoria 3800, Australia

Received December 27, 2000

Substitution of the weakly binding aqua ligand in $[Cu(tren)OH_2]^{2+}$ and $[Cu(tpa)OH_2]^{2+}$ (tren = tris(2-aminoethyl)-amine; tpa = tris(2-pyridylmethyl)amine) by a cyano ligand on ferricyanide results in the assembly of heteropolynuclear cations around the cyanometalate core. In water, the reduction of the Fe^{III} core to Fe^{II} generates complexes that feature heteropolycations in which ferrocyanide is encapsulated by the Cu^{II} moieties: $[\{Cu(tpa)CN\}_6Fe][ClO_4]_8 \cdot 3H_2O$ **1**, $[\{Cu(tren)CN\}_6Fe][ClO_4]_8 \cdot 10H_2O$ **2**, $[\{Cu(tren)CN\}_6Fe][Fe(CN)_6]_2[ClO_4]_2 \cdot 15.8H_2O$ **3**, and $[\{Cu(tren)CN\}_6Fe][\{Cu(tren)CN\}_4Fe(CN)_2][Fe(CN)_6]_4 \cdot 6DMSO \cdot 21H_2O$ **4**. The formation of discrete molecules, in preference to extended networks or polymeric structures, has been encouraged through the use of branched tetradentate ligands in conjunction with copper(II), a metal center with the propensity to form five-coordinate complexes. Complex **3** crystallizes in the monoclinic space group $P2_1/c$ (#14) with $a = 14.8674(10)$, $b = 25.9587(10)$, $c = 27.5617(10)$ Å, $\beta = 100.8300(10)$ °, and $Z = 4$, and it is comprised of almost spherical heptanuclear cations, $[\{Cu(tren)CN\}_6Fe]^{8+}$, whose charge is balanced by two ferricyanide and two perchlorate counteranions. Complex **4** crystallizes in the triclinic space group $P1$ (# 1) with $a = 14.8094(8)$, $b = 17.3901(7)$, $c = 21.1565(11)$ Å, $\alpha = 110.750(3)$, $\beta = 90.206(2)$, $\gamma = 112.754(3)$ °, and $Z = 1$, and it is comprised of the heptanuclear $[\{Cu(tren)CN\}_6Fe]^{8+}$ cation and pentanuclear $[\{Cu(tren)CN\}_4Fe(CN)_2]^{4+}$ cation, whose terminal cyano ligands are oriented trans to each other. The charge is balanced exclusively by ferricyanide counteranions. In both complexes, H-bonding interactions between hydrogens on primary amines of the tren ligand, terminal cyano groups of the ferricyanide counterions, and the solvent of crystallization generate intricate 3D H-bonding networks.

Introduction

Hexacyanometalates have been employed extensively as building blocks for constructing extended-array multimetallic assemblies with novel structural features and physicochemical properties.[1−6] Recognition of the ability of cyanide groups to bridge metal centers has led to the use of hexacyanometalates as templates for the preparation of heterometallic coordination polymers having one-dimensional (1-D), two-dimensional (2-D), or three-dimensional (3-D) extended array structures.[3,4,7−24] Despite the significant recent advances, magnetostructural correlations have proved to be elusive in some cases due to the inability to obtain crystals suitable for X-ray structural deter-

* To whom correspondence should be addressed. Phone: 61 3 9905 45 26. Fax: 61 3 9005 4597. Email: leone.spiccia@sci.monash.edu.au.
† School of Chemistry, Monash University.
‡ Department of Physics, Monash University.

(1) Klenze, H.; Kanellalopulos, B.; Tragester, G.; Eysel, H. *J. Chem. Phys.* **1980**, *72*, 5819.
(2) Gadet, V.; Bujoli-Doeuff, M.; Force, L.; Verdaguer, M.; El Malkhi, K.; Deroy, A.; Besse, J. P.; Chappert, C.; Veillet, P.; Renard, J. P.; Beauvillain, P. *Magnetic Molecular Materials*; Gatteschi, D., Kahn, O., Miller, J. S., Palacio, F., Eds.; (NATO ASI Series E); Kluwer Academic: Dordrecht, The Netherlands, 1991; Vol. 198, p 281.
(3) Gadet, V.; Mallah, T.; Castro, I.; Verdaguer, M. *J. Am. Chem. Soc.* **1992**, *114*, 9213.
(4) Mallah, T.; Thiebaut, S.; Verdaguer, M.; Veillet, P. *Science* **1993**, *262*, 1554.
(5) Entley, W. R.; Girolami, G. S. *Inorg. Chem.* **1994**, *33*, 5165.
(6) Kahn, O. *Adv. Inorg. Chem.* **1995**, *43*, 179.
(7) Ferlay, S.; Mallah, T.; Ouahés, R.; Veillet, P.; Verdaguer, M. *Inorg. Chem.* **1999**, *38*, 229.
(8) Sato, O.; Einaga, Y.; Fujishima, A.; Hashimoto, K. *Inorg. Chem.* **1999**, *38*, 4405.
(9) Ohba, M.; Maruono, N.; Okawa, H.; Enoki, T.; Latour, J. M. *J. Am. Chem. Soc.* **1994**, *116*, 11566.
(10) Ohba, M.; Okawa, H.; Ito, T.; Ohto, A. *J. Chem. Soc., Chem. Commun.* **1995**, 1545.
(11) Ferley, S.; Mallah, T.; Ouahés, R.; Veillet, P.; Verdaguer, M. *Nature* **1995**, *378*, 701.
(12) Miyasaka, H.; Matsumoto, N.; Okawa, H.; Re, N.; Gallo, E.; Floriani, C. *Angew. Chem., Int. Ed. Engl.* **1995**, *34*, 1446.
(13) Miyasaka, H.; Matsumoto, N.; Okawa, H.; Re, N.; Gallo, E.; Floriani, C. *J. Am. Chem. Soc.* **1996**, *118*, 981.
(14) Ferlay, S.; Mallah, T.; Vaissermann, J.; Bartolome, F.; Veillet, P.; Verdaguer, M. *J. Chem. Soc., Chem. Commun.* **1996**, 2481.
(15) Salah El Fallah, M.; Rentschler, E.; Caneschi, A.; Sessoli, R.; Gatteschi, D. *Angew. Chem., Int. Ed. Engl.* **1996**, *35*, 1947.
(16) Re, N.; Gallo, E.; Floriani, C.; Miyasaka, H. Matsumoto, N. *Inorg. Chem.* **1996**, *35*, 5964 and 6004.
(17) Michaut, C.; Ouahab, L.; Bergerat, P.; Kahn, O.; Bousseksov, A. *J. Am. Chem. Soc.* **1996**, *118*, 3650.
(18) Ohba, M.; Fukita, N.; Okawa, H. *J. Chem. Soc., Dalton Trans.* **1997**, 1733. Ohba, M.; Okawa, H.; Fukita, N.; Hashimoto, Y. *J. Am. Chem. Soc.* **1997**, *119*, 1011.
(19) Verdaguer, M.; Siberchicot, B.; Eyert, V. *Phys. Rev. B*: **1997**, *56*, 8959.
(20) Miyasaka, H.; Okawa, H.; Miyasaki, A.; Enoki, T. *Inorg. Chem.* **1998**, *37*, 4878.
(21) Colacio, E.; Dominguez-Vera, J. M.; Ghazi, M.; Kivekäs, R.; Lloret, F.; Moreno, J. M. *Chem. Commun.* **1999**, 987. Colacio, E.; Dominguez-Vera, J. M.; Ghazi, M.; Kivekäs, R.; Moreno, J. M.; Pajuner, A. *J. Chem. Soc., Dalton Trans.* **2000**, 505.

10.1021/ic001452f CCC: $20.00
Published on Web 07/26/2001

mination. To gain further insight into the structure and properties of such assemblies, recent research has also focused on the design of discrete polynuclear entities (eg., nuclearity < 20).[27−38] In certain cases, the discrete entities can be viewed as building blocks to the frameworks that exhibit bulklike ferromagnetic properties and, therefore, allow information to be obtained about the transition from molecular to bulklike magnetic behavior.

One synthetic strategy to discrete heteropolynuclear assemblies has involved the capping of cyano groups on hexacyanometalate anions, such as $[Fe(CN)_6]^{3-/4-}$ and $[Cr(CN)_6]^{3-}$, with appropriate transition metal complexes.[27−35] To generate discrete entities, one coordination site on the metal complex should generally be occupied by a weakly binding ligand that is capable of being displaced by a cyano group from the hexacyanometalate. For example, in the case of metal centers that adopt octahedral coordination (eg., Ni^{II} and Mn^{II}), heptanuclear cations have been formed by the reaction of complexes of a strongly binding pentadentate ligand with the hexacyanometalate (in a 6:1 molar ratio). The first complex of this type to be reported, $[\{Ni(tetren)(CN)\}_6Cr][ClO_4]_9$ (tetren = tetraethylenepentamine), consisted of a $[Cr(CN)_6]^{3-}$ capped by six $[Ni(tetren)]^{2+}$ moieties.[29] Further examples of these types of complexes, which range from trinuclear complexes to more elaborate, but still discrete entities, have been appeared in recent years.[30−38]

Our own studies in this area have been prompted by the fact that discrete heptanuclear complexes assembled around hexacyanometalate are still relatively rare, and few such complexes have been characterized by X-ray crystallography. The structural characteristics of discrete heteropolynuclear complexes incorporating hexacyanometalates remain relatively undeveloped. We have shown that the reaction of the Cu^{II} complex of the strongly coordinating tetradentate ligand tris(2-pyridylmethyl)amine (tpa) with ferricyanide results in the encapsulation of hexacyanoferrate core by six $[Cu(tpa)]^{2+}$ moieties and formation of the heptanuclear complex, $[\{Cu(tpa)CN\}_6Fe][ClO_4]_8\cdot 3H_2O$ **1**.[31] In this paper, we report three further discrete heteropolynuclear assemblies, formed by reacting ferricyanide salts with $[Cu(tren)OH_2]^{2+}$ (tren = tris(2-aminoethyl)amine), and elaborate further on novel structural features of **1**. Apart from the assembly of heptanuclear cations and in one case a pentanuclear cation, H-bonding interactions between cations, anions, and solvate molecules have generated novel extended networks.

Results and Discussion

Synthesis. The heteropolynuclear complexes, $[\{Cu(tpa)CN\}_6Fe][ClO_4]_8\cdot 3H_2O$ **1**, $[\{Cu(tren)CN\}_6Fe][ClO_4]_8\cdot 10H_2O$ **2**, and $[\{Cu(tren)CN\}_6Fe][Fe(CN)_6]_2[ClO_4]_2\cdot 15.8H_2O$ **3** were formed by the reaction of $[Cu(tren)OH_2]^{2+}$ and $[Cu(tpa)OH_2]^{2+}$ with $[Fe(CN)_6]^{3-}$ in water. The use of the tetradentate tren and tpa ligands in conjunction with Cu^{II}, a metal center capable of forming five-coordinate complexes, has facilitated the formation of discrete heterometallic molecules, in preference to extended coordination networks or polymeric structures. These assemblies are generated through the displacement of a weakly binding ligand (solvent) from the Cu(II) center by the cyano groups of the hexacyanometalate.

Complexes **1** and **2** were formed by dropwise addition of $K_3[Fe(CN)_6]$ ($^n/_6$ mols) to the in situ generated $[Cu(tpa)(OH_2)]^{2+}$ and $[Cu(tren)(OH_2)]^{2+}$ complexes (*n* mols). Recrystallization from hot water gave purple crystals of **1** (X-ray structure has been communicated[31]). Reaction of $[Cu(tren)OH_2][ClO_4]_2$ (2*n* mols) with $K_3[Fe(CN)_6]$ (*n* mols), in the presence of an excess of the oxidant, $K_2S_2O_8$, gave a dark green solution from which dark green needles of $[\{Cu(tren)CN\}_6Fe^{II}][Fe^{III}(CN)_6]_2[ClO_4]_2\cdot 15.8H_2O$ **3** deposited on slow evaporation. The X-ray crystal structure confirmed the formation of heptanuclear $[\{Cu(tren)CN\}_6Fe^{II}]^{8+}$ cations (see below). The oxidant was unable to prevent the reduction of the iron center in the encapsulated hexacyanoferrate. Indeed, the corresponding Fe^{III} $[\{Cu(tren)CN\}_6Fe^{II}]^{9+}$ cation could only be isolated through the use of acetonitrile, an aprotic solvent.[39]

Recrystallization of the trinuclear Fe^{III} complex, $[\{Cu(tren)CN\}_4Fe(CN)_2](ClO_4)$,[39] from DMSO afforded $[\{Cu(tren)CN\}_6Fe^{II}][\{Cu(tren)CN\}_4Fe^{II}(CN)_2][Fe^{III}(CN)_6]_4.6DMSO\cdot 21H_2O$ **4**, a compound containing both heptanuclear and pentanuclear $Fe^{II}-Cu^{II}$ cations. The Fe:Cu ratio in **4** (10:6) is similar to that of the starting trinuclear complex.

Infrared Spectra. The infrared spectra of **1**−**4** exhibit the bands expected for the ligands and counterions. The ν_{CN} stretching region (2000−2200 cm^{-1}) contains information that can allow the iron oxidation state in the hexacyanoferrate to be assigned and the presence of cyanide bridges ascertained. In general, terminal CN stretches occur at ca. 2110 and 2040 cm^{-1} when attached to Fe^{III} and Fe^{II}, respectively. On the other hand, the respective locations of bridging CN groups are typically >2150 cm^{-1} [27,28,40,41] and ca. 2100 cm^{-1}.[41] Although unambiguous assignment can prove to be difficult, important conclusions can be drawn. For **1** and **2**, the shift in the ν_{CN} stretch from 2042 cm^{-1} in $K_4[Fe(CN)_6]$ to 2109 cm^{-1} in **1** and 2106 cm^{-1} in **2** indicates the assembly of $Fe^{II}-CN-Cu^{II}$ bridging units around the ferrocyanide core. Complex **3** exhibits a band at 2100 cm^{-1} which, from its correspondence to bands exhibited by **1**

(22) Smith, J. A.; Galan-Mascaros, J.-R.; Clerac, R.; Dunbar, K. R. *Chem. Commun.* **2000**, 1077.
(23) Zhang, S.-W.; Fu, D.-G.; Sun, W.-Y.; Hu, Z.; Yu, K.-B.; Tang, W.-X. *Inorg. Chem.* **2000**, *39*, 1142.
(24) Zhau, S.; Guo, D.; Zhang, X.; Du, C.; Zhu, Y.; Yan, Y. *Inorg. Chim. Acta* **2000**, *298*, 57.
(25) Shek, I. P. Y.; Wong, W.-Y.; Lau, T.-C. *New. J. Chem.* **2000**, *24*, 733.
(26) Kou, H.-Z.; Bu, W.-M.; Gao, S.; Liao, D.-Z.; Jiang, Z.-H.; Yan, S.-P.; Fan, Y.-G.; Wang, G.-L. *J. Chem. Soc., Dalton Trans.* **2000**, 2996.
(27) Scott, M.; Lee, S.; Holm, R. *Inorg. Chem.* **1994**, *33*, 4651.
(28) Scott, M.; Holm, R. *J. Am. Chem. Soc.* **1994**, *116*, 11357.
(29) Mallah, T.; Auberger, C.; Verdaguer, M.; Veillet, P. *Chem. Commun.* **1995**, 61.
(30) Sculler, A.; Mallah, T.; Verdaguer, M.; Nivorozkhin, A.; Tholence, J.; Veillet, P. *New J. Chem.* **1996**, *20*, 1.
(31) Parker, R. J.; Hockless, D. C. R.; Moubaraki, B.; Murray, K. S.; Spiccia, L. *Chem. Commun.* **1996**, 2789.
(32) Van Langenberg, K.; Batten, S. R.; Berry, K. J.; Hockless, D. C. R.; Moubaraki, B.; Murray, K. S. *Inorg. Chem.* **1997**, *36*, 5006.
(33) Bernhardt, P. V.; Martinez, M. *Inorg. Chem.* **1999**, *38*, 424.
(34) Arrio, M.-A., Sculler, A.; Saintctavit, Ph.; Cartier de Moulin, Ch.; Mallah, T.; Verdaguer, M. *J. Am. Chem. Soc.* **1999**, *121*, 6414.
(35) Verdaguer, M.; Bleuzen, A.; Marvaraud, V.; Vaissermann, J.; Seuleiman, M.; Desplanches, C.; Scuiller, A.; Train, C.; Garde, R.; Gally, G.; Momenech, C.; Rosenman, I.; Veillet, P.; Cartier, C.; Villain, F. *Coord. Chem. Rev.* **1999**, *190−192*, 1023.
(36) Larianova, J.; Gross, M.; Pilkington, M.; Audres, H.; Stoeckli-Evans, H.; Güdel, H. U.; Descurtins, S. *Angew. Chem., Int. Ed.* **2000**, *39*, 1605.
(37) Zhong, Z. J.; Seino H.; Mizobe, Y.; Hidai, M.; Fujishima, A.; Ohkoshi S.; Hashimoto, K. *J. Am. Chem. Soc.* **2000**, *122*, 2952. Zhong, Z. J.; Seino H.; Mizobe, Y.; Hidai, M.; Verdaguer, M.; Ohkoshi S.; Hashimoto, K. *Inorg. Chem.* **2000**, *39*, 5095.
(38) Sra, A. K.; Rombaut, G.; Lahitete, F.; Golhen, S.; Ouahab, L.; Mathoniere, C.; Yakhmi, J. V.; Kahn, O. *New J. Chem.* **2000**, *24*, 871.
(39) Parker, R. J. Ph.D. Dissertation, Monash University, Victoria, Australia, 1999.
(40) Morpurgo, G.; Mosini, V.; Porta, P.; Dessy, G.; Fares V. *J. Chem. Soc., Dalton Trans.* **1981**, 111.
(41) Nakamoto, K. *Infrared and Raman Spectra of Inorganic and Coordination Compounds*; 4 ed.; Wiley-Interscience: New York, 1978.

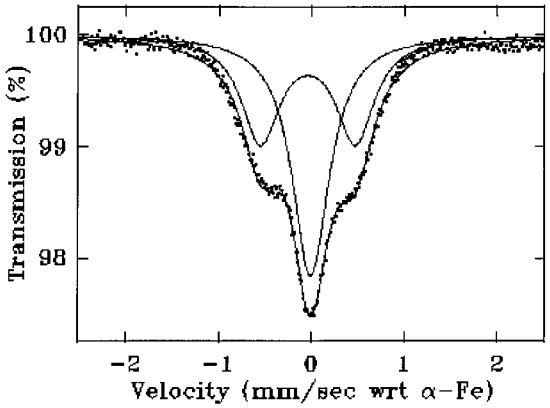

Figure 1. Mössbauer spectrum of **3**, recorded at 5 K. The solid line represents a least-squares fit to the data based on the superposition of a singlet due to the Fe^{II} heptanuclear cation and doublet due the ferricyanide counterions.

and **2** and the X-ray structure (see below), can be attributed to the intermetallic stretch in $[\{Cu(tren)CN\}_6Fe]^{8+}$. The band at 2148 cm^{-1} can be assigned as the ν_{CN} stretch of the ferricyanide counteranions. A positive shift of 35 cm^{-1}, relative to the band for $K_3[Fe(CN)_6]$, most likely results from H-bonding interactions between the water molecules and counteranions and/or electronic interactions between Cu^{II} cations on the periphery of the Fe−Cu cluster and $[Fe(CN)_6]^{3-}$ anions. The band for $[Fe(CN)_6]^{3-}$ is sensitive to the countercation[40] and in the case of **3** falls between those observed for the $[Cu(OH_2)_6]^{2+}$ (2170 cm^{-1}) and K^+ (2115 cm^{-1}) salts.

Complex **4** displays a band at 2043 cm^{-1} due to a terminal ν_{CN} stretch in the pentanuclear cation with a central Fe^{II} core $[\{Cu(tren)CN\}_4Fe(CN)_2]^{4+}$ (cf. 2042 cm^{-1} for $K_4[Fe(CN)_6]$) and a second band at 2080 cm^{-1}, which is attributable to the bridging ν_{CN} stretch of the pentanuclear cation. Bands at 2100 and 2109 cm^{-1} cannot be assigned unambiguously but since their locations compare well to the bridging CN stretches in **1**−**4** (2100−2110 cm^{-1}) and the terminal CN stretch of $K_3[Fe(CN)_6]$, one is due to the bridging ν_{CN} stretch in $[\{Cu(tren)CN\}_6Fe]^{8+}$ and the other to the terminal CN stretch of the hexacyanoferrate(III) counteranions. The fact that the latter is at a lower wavenumber (2109 cm^{-1}), than is the case for **3** (2148 cm^{-1}), supports the notion that the higher terminal CN stretch for **3** is due to hydrogen bonding involving water molecules and not due to electronic interactions between Cu^{II} and $[Fe(CN)_6]^{3-}$ ions.

Mössbauer Spectroscopy. The Mössbauer spectra for **1** and **2**, recorded at 81 K, exhibit strong, narrow single lines at $\delta = -0.05(1)$ mm s^{-1} (fwhm 0.27(1) mm s^{-1}) and $\delta = 0.20(2)$ mm s^{-1} (fwhm 0.32(1) mm s^{-1}), respectively.[31] This is indicative of a unique low-spin Fe^{II} environment with a symmetrical ligand field, leading to zero quadrupole splitting.[42] The Mössbauer spectrum of **3**, recorded at 5 K (Figure 1), consists of a pseudo-triplet which can be interpreted as the superimposition of one doublet ($\delta = -0.04(1)$ mm s^{-1}, $\Delta E = 1.02(1)$ mm s^{-1}, fwhm 0.51 mm s^{-1}), due to the ferricyanide counteranions, and one singlet ($\delta = -0.01(1)$ mm s^{-1}, fwhm 0.48 mm s^{-1}), due to the Fe^{II} of the heptanuclear cation. The area ratio was 48(3)%: 52(3)%. Minor deviations between observed and fitted spectra suggest the presence of a small amount of a different hexacyanoferrate material. Fitting of the data at 81 K to the same model gave $\delta = -0.03(1)$ mm s^{-1}, $\Delta E = 1.04(1)$ mm s^{-1}, fwhm 0.55 mm s^{-1} for the doublet and $\delta = -0.01(1)$ mm s^{-1}, fwhm 0.42 mm s^{-1} for the singlet, with an area ratio of 51(3)%: 49(3)%. The apparent change in linewidth of the singlet is probably due to a change in an unresolved quadrupole splitting. The larger quadrupole splitting for the ferricyanide counterions, than observed in potassium ferricyanide ($\delta = -0.00$ mm s^{-1}, $\Delta E = 0.47$ mm s^{-1}),[42] may be related to the extensive involvement of these anions in H-bonding interactions (see below).

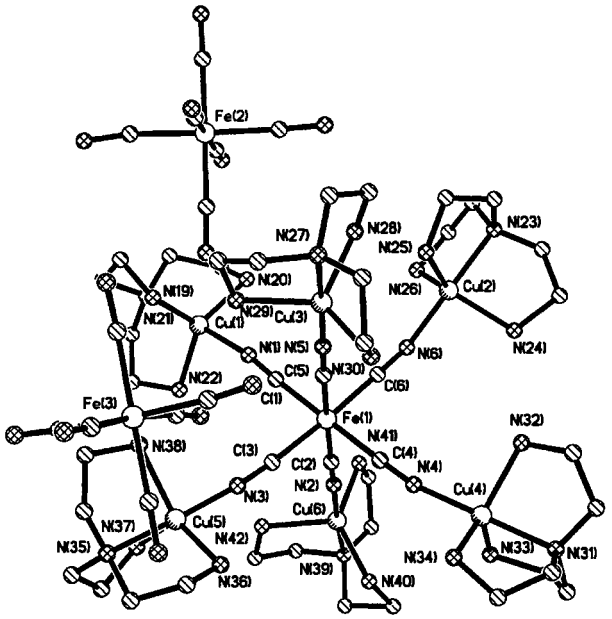

Figure 2. ORTEP diagram of the heptanuclear complex $[\{Cu(tren)CN\}_6Fe]^{8+}$ of **3** showing the atom labeling scheme and 50% thermal vibrational ellipsoids. Hydrogen atoms have been omitted for clarity.

X-ray Crystal Structures. Complex **3** exhibits an almost spherical heptanuclear cation formed by the encapsulation of one $[Fe(CN)_6]^{4-}$ core by six $[Cu(tren)]^{2+}$ units (Figure 2) whose charge is balanced by two perchlorate and two $[Fe(CN)_6]^{3-}$ anions, rather than exclusively by perchlorate anions as is the case for **1**. The cation, the 20 surrounding water molecules, and the ferricyanide anions form a complex three-dimensional H-bonding network (discussed later).

The Fe^{II} center of the heptanuclear core and the Fe^{III} of the ferricyanide counteranions are close to octahedral, with the *cis*-C−Fe−C angles and the *trans*-C−Fe−C angles close to 90° and 180°, respectively (see Table 1). The Fe−C bond distances, Fe−C−N angles, and Cu−N(cyano) bond distances are in accordance with literature values for related Fe^{II}, Fe^{III}−Cu^{II}, or Cu^{II} complexes, including discrete heteropolynuclear complexes and extended networks.[27,28,41,43−48] The Fe···Cu distances (4.90−4.99 Å) are at the lower end of Fe···Cu separations reported for discrete molecules and lattice networks[27,28,41,45,51−54] and are similar to those in **1**. The variation in Cu−N−C angles from significantly bent (163.4(9)°) to near linear (177(1)°) is

(42) Greenwood, N. N.; Gibb, T. C. *Mössbauer Spectroscopy*; Chapman & Hall: London, 1971.

(43) Lee, S.; Scott, M.; Munck, E.; Kauffmann, K.; Holm, R. *J. Am. Chem. Soc.* **1994**, *116*, 401.

(44) Morpurgo, G.; Mosini, V.; Porta, P. *J. Chem. Soc., Dalton Trans.* **1980**, 1272.

(45) Kou, H.; Liao, D.; Cheng, P.; Jiang, Z.; Yan, S.; Wang, G.; Yao, X.; Wang, H. *J. Chem. Soc., Dalton Trans.* **1997**, 1503.

(46) Lu, Z.; Duan, C.; Tian, Y.; Wu, Z.; You, J. Z., Z.; Mak, T. *Polyhedron* **1997**, *16*, 909.

(47) Chen, Z. N.; Wang, J. L.; Qui, J.; Miao, F. M.; Tang, W. X. *Inorg. Chem.* **1995**, *34*, 2255.

(48) Wu, M. F.; Chen, Z. W.; Qui, J.; Tang, W. X. *Chin. Chem. Lett.* **1994**, *5*, 713.

(49) Zou, J.; Xu, Z.; Huang, X.; Zhang, W.; Shen, X.; Yu, Y. *J. Coord. Chem.* **1997**, *42*, 55.

Table 1. Selected Bond Distances (Å) and Angles (Deg) for **3**

Bond Distances			
Fe(1)−C(1)	1.90(1)	Cu(2)−N(6)	1.94(1)
Fe(1)−C(2)	1.89(1)	Cu(2)−N(23)	2.03(1)
Fe(1)−C(3)	1.90(1)	Cu(2)−N(24)	2.05(1)
Fe(1)−C(4)	1.89(1)	Cu(2)−N(25)	2.06(1)
Fe(1)−C(5)	1.88(1)	Cu(3)−N(27)	2.051(9)
Fe(1)−C(6)	1.87(1)	Cu(3)−N(28)	2.10(1)
Cu(1)−N(1)	1.951(9)	Cu(3)−N(29)	2.058(8)
Cu(1)−N(19)	2.056(7)	Cu(3)−N(30)	2.050(9)
Cu(1)−N(20)	2.07(1)	Cu(4)−N(4)	1.950(9)
Cu(1)−N(21)	2.07(1)	Cu(4)−N(31)	2.054(9)
Cu(1)−N(22)	2.04(1)	Cu(4)−N(32)	2.08(1)
Cu(2)−N(26)	2.08(1)	Cu(4)−N(33)	2.08(1)
Cu(3)−N(5)	1.93(1)	Cu(4)−N(34)	2.06(1)
Cu(5)−N(3)	1.93(1)	Cu(6)−N(2)	1.93(1)
Cu(5)−N(35)	2.040(8)	Cu(6)−N(39)	2.01(1)
Cu(5)−N(36)	2.01(1)	Cu(6)−N(40)	2.00(2)
Cu(5)−N(37)	2.11(1)	Cu(6)−N(41)	2.03(1)
Cu(5)−N(38)	2.096(8)	Cu(6)−N(42)	2.14(1)
Fe(1)···Cu(1)	4.975	Fe(1)···Cu(4)	4.969
Fe(1)···Cu(2)	4.909	Fe(1)···Cu(5)	4.959
Fe(1)···Cu(3)	4.983	Fe(1)···Cu(6)	4.983
Bond Angles			
Fe(1)−C(1)−N(1)	177.0(9)	C(4)−Fe(1)−C(6)	89.9(4)
Fe(1)−C(2)−N(2)	178.6(9)	C(5)−Fe(1)−C(6)	89.4(4)
Fe(1)−C(3)−N(3)	176.9(10)	Cu(1)−N(1)−C(1)	171.1(9)
Fe(1)−C(4)−N(5)	178.5(9)	Cu(2)−N(6)−C(6)	163.4(9)
Fe(1)−C(5)−N(5)	178.2(9)	Cu(3)−N(5)−C(5)	176.0(9)
Fe(1)−C(6)−N(6)	176.6(9)	Cu(4)−N(4)−C(4)	167.4(9)
C(1)−Fe(1)−C(2)	89.1(4)	Cu(5)−N(3)−C(3)	170.0(9)
C(1)−Fe(1)−C(3)	89.1(4)	Cu(6)−N(2)−C(2)	176.8(10)
C(1)−Fe(1)−C(4)	178.5(4)	N(1)−Cu(1)−N(19)	178.0(3)
C(1)−Fe(1)−C(5)	91.1(4)	N(1)−Cu(1)−N(20)	97.4(4)
C(1)−Fe(1)−C(6)	88.7(4)	N(1)−Cu(1)−N(21)	95.7(4)
C(2)−Fe(1)−C(3)	91.7(4)	N(1)−Cu(1)−N(22)	94.3(4)
C(2)−Fe(1)−C(4)	90.4(4)	N(19)−Cu(1)−N(20)	84.6(4)
C(2)−Fe(1)−C(5)	179.0(4)	N(19)−Cu(1)−N(21)	83.6(3)
C(2)−Fe(1)−C(6)	89.6(4)	N(19)−Cu(1)−N(22)	84.3(4)
C(3)−Fe(1)−C(4)	92.3(4)	N(20)−Cu(1)−N(21)	120.9(4)
C(3)−Fe(1)−C(5)	89.3(4)	N(20)−Cu(1)−N(22)	118.6(5)
C(3)−Fe(1)−C(6)	177.4(4)	N(21)−Cu(1)−N(22)	117.4(5)
C(4)−Fe(1)−C(5)	89.4(4)		

larger than in related discrete molecules.[27,28,43] This may be due to steric interactions between the tren ligands on adjacent Cu^{II} centers and the presence of H-bonding interactions (see later). Significantly, in the trinuclear complex, $[\{Cu(tren)(CN)\}_2Fe(CN)_4]\cdot 12H_2O$,[46−49] which has an Fe^{II} center bridging two $[Cu(tren)]^{2+}$ units and a 3D H-bonded network, the Cu−N−C(cyano) bond angle (144°) is even lower than what is observed for **3**. It should be stressed that large deviations from linearity are observed in lattice coordination networks, which exhibit Cu−N−C angles of 107° to 174°.[40,44,45,48]

The $[Cu(tren)]^{2+}$ units in **3** adopt a distorted TBP geometry, where the primary amine groups on each tren ligand occupy the equatorial positions around the Cu^{II} center and the tertiary amine nitrogen located in the axial position trans to the cyano bridge. Within the equatorial plane there are significant variations in the Cu−N distances (2.01(1)−2.14(1) Å) and N−Cu−N angles (105.5(5)−135.4(7)°). Despite this, the N(am)−Cu−N(CN) angles in all Cu^{II} moieties are close to linear (176.7(4)−179.1(4)°), as found in regular TBP geometry. One interesting feature of **3** is that the geometry around some Cu^{II} centers is almost regular while other Cu^{II} centers are significantly distorted. The range in τ values[50] from 0.70 to 0.92 for Cu(6) and Cu(1), respectively, highlights this variation. For Cu(1), the N−Cu−N bond angles in the equatorial N_3 plane (117.4(5)−120.9(4)°) span a tight range around 120°, as expected for regular TBP. In contrast, the angles around Cu(6) show greater deviation (105.5(5)−135.4(7)°). The formation of three five-membered chelate rings involving each arm of the tren ligand and the Cu^{II} center results in acute H_2N−Cu−N(amine) angles and the displacement of the Cu centers (by 0.18−0.22 Å) away from the N_3 plane of the primary amines toward the cyano ligand. Slightly greater displacements are evident in **1**.

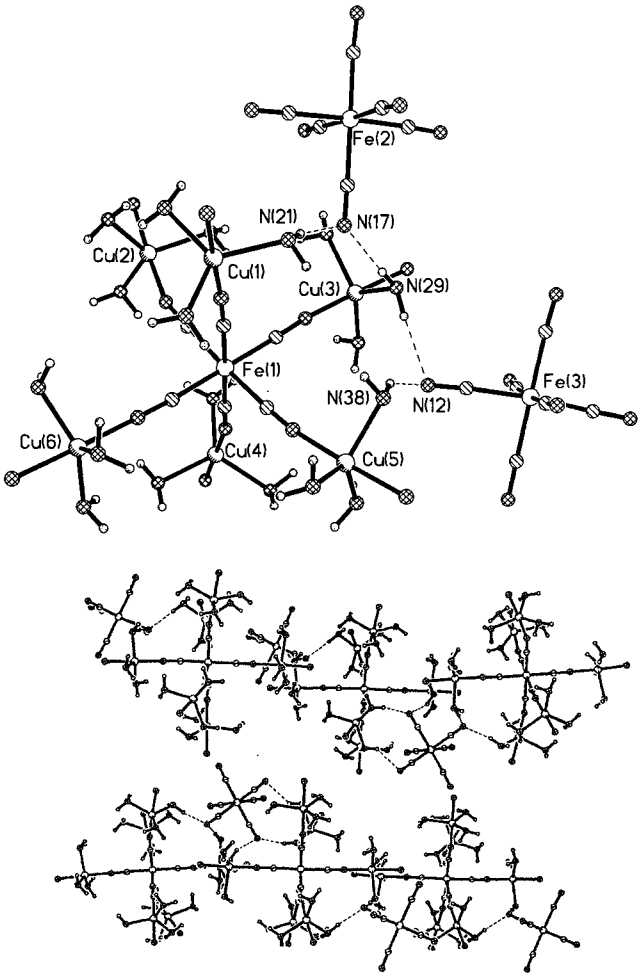

Figure 3. (a) A diagram of **3** showing the H-bonding interactions between the heptanuclear cation and ferricyanide counteranions. (b) Extended packing of the H-bonding in **3** which shows the formation of parallel chains of ferricyanide anions and heptanuclear cations. The peripheral atoms of the tren ligand, water molecules, and perchlorate anions have been removed for clarity.

The elaborate H-bonding network that connects the ferricyanide anions and the heptanuclear cation and involves the water of crystallization and some tren primary amines (see Figure 3) is an important feature of **3**. The establishment of the network seems to be aiding crystallization. In particular, the primary amines of the ligands capping Cu(1), Cu(3), and Cu(5) interact with the nitrogen atom of one terminal cyanide on each ferricyanide anion. The N(17) atom of ferricyanide anion, Fe(2), forms two H-bonds, one with a hydrogen on N(21) of the Cu(1) moiety (N(21)···N(17), 3.163 Å), and the other with a

(50) Addison, A. W.; Rao, T. N.; Reedijk, J.; van Rijn, J.; Verschoor, G. C. *J. Chem. Soc., Dalton Trans.* **1984**, 1349.
(51) Miyasaka, H.; Matsumoto, N.; Re, N.; Gallo, E.; Floriani, C. *Inorg. Chem.* **1997**, *36*, 670.
(52) Re, N.; Crescenzi, R.; Floriani, C.; Miyasaka, H.; Matsumoto, N. *Inorg. Chem.* **1998**, *37*, 2717.
(53) Duggan, M.; Ray, N.; Hathaway, B.; Tomlinson, G.; Brint, P.; Pelin, K. *J. Chem. Soc., Dalton Trans.* **1980**, 1342.
(54) Hathaway, B. J. In *Comprehensive Coordination Chemistry*; Wilkinson, G., Gillard, R. D., McCleverty, J. A., Eds.; Pergamon Press: Oxford, 1987; Vol. 5, pp 533−774.

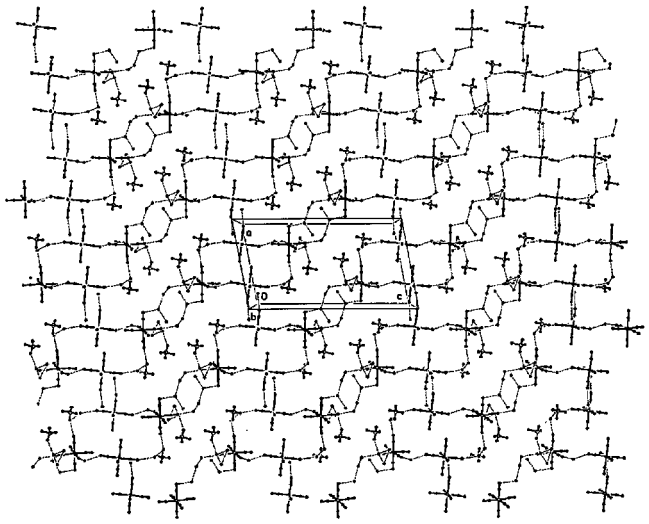

Figure 4. An extended packing diagram of the hydrogen bonded network in **3** formed with the water molecules, perchlorate anions, and ferricyanide counteranions. The heptanuclear cation has been omitted to highlight the formation of diagonal zigzag chains when viewing down the *b* axis.

hydrogen on N(29) coordinated to Cu(3) (N(29)···N(17), 2.987 Å). The N(12) from the other ferricyanide anion, Fe(3), is similarly involved in two way H-bonding to a hydrogen on N(38) of Cu(5) (distance 3.129 Å) and a hydrogen on N(29) of the Cu(3) moiety (distance 3.011 Å). Consequently, the primary amine N(29) hydrogen bonds with a cyano group from each hexacyanoferrate anion, N(12) on Fe(3) and N(17) on Fe(2). This effectively sandwiches the Cu(3)−tren moiety between the two counteranions, thereby generating intermolecular separations of 8.036 Å for Fe(1)···Fe(2), 9.018 Å for Fe(1)···Fe(3), and 9.704 Å for Fe(2)···Fe(3). The net result of these H-bonding interactions is the generation of parallel chains of ferricyanide anions and heptanuclear cations, which are clearly apparent in the extended packing shown in Figure 4.

The extended packing viewed down the *b* axis reveals that the ferricyanide anions and water molecules (Figure 4) form diagonal zigzag chains. On each chain, there is a pseudo-rectangular segment with steplike diamonds, which is made up of six water molecules and four cyanides. These extend from the two opposing corners of each pseudo-rectangle. Ferricyanide anions present at each opposing corner link the rectangles and steplike diamonds into a 2D network. Additional H-bonding between anions and cations (vide supra) running approximately perpendicular to these zigzag chains extends the network in the third dimension.

An account of the structure of $[\{Cu(tpa)CN\}_6Fe][ClO_4]_8 \cdot 3H_2O$ (**1**) has been communicated,[31] and discussion here is focused on some novel packing features. Figure 5(a) shows the quasi-spherical $[\{Cu(tpa)CN\}_6Fe]^{8+}$ units formed by encapsulation of $[Fe(CN)_6]^{4-}$ by six $[Cu(tpa)]^{2+}$ units. The extended packing of **1**, viewed down the *a* axis, shows that the spherical cations stack in regular columns, which are arranged in a staggered orientation (Figure 5(b)). When viewed down the *c* axis, the regular stacking of the heptanuclear cations that creates tubular cavities that host the perchlorate counteranions (Figure 5(c)) is clearly evident.

The structure of $[\{Cu(tren)CN\}_6Fe][\{Cu(tren)CN\}_4Fe(CN)_2][Fe(CN)_6]_4 \cdot 6DMSO \cdot 21H_2O$, **4**, confirms the cocrystallization of three types of hexacyanoferrates, viz., heptanuclear cations, $[\{Cu(tren)CN\}_6Fe^{II}]^{8+}$, pentanuclear cations, $[\{Cu(tren)CN\}_4Fe^{II}(CN)_2]^{4+}$, and ferricyanide counteranions. In the heptanuclear

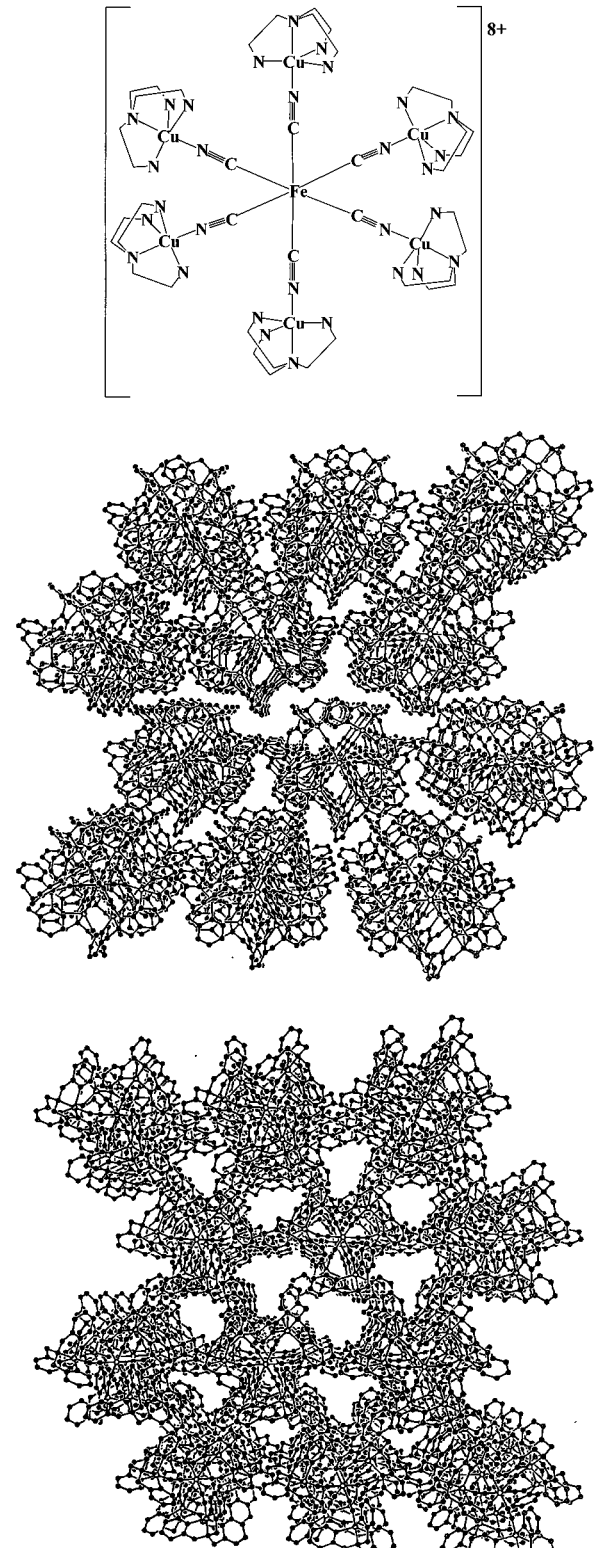

Figure 5. (a) Diagram of the heptanuclear complex, $[\{Cu(tpa)CN\}_6Fe]^{8+}$ of **1** (representation of pyridyl rings of tpa ligand simplified for clarity).[31] Extended packing of **1** viewed down the: (b) *a* axis, showing the heptanuclear cations stacking in staggered columns, and (c) *c* axis. The hydrogen atoms, perchlorate anions, and water molecules have been omitted for clarity. The perchlorate anions reside in the tubular cavities.

cation, $[Fe^{II}(CN)_6]^{4-}$ is encapsulated by six $[Cu(tren)]^{2+}$ units forming an almost spherical complex (Figure 6(a)), which is very similar to that found in **3**. In the pentanuclear cation, the four $[Cu(tren)]^{2+}$ moieties bind to four equatorial cyanides on

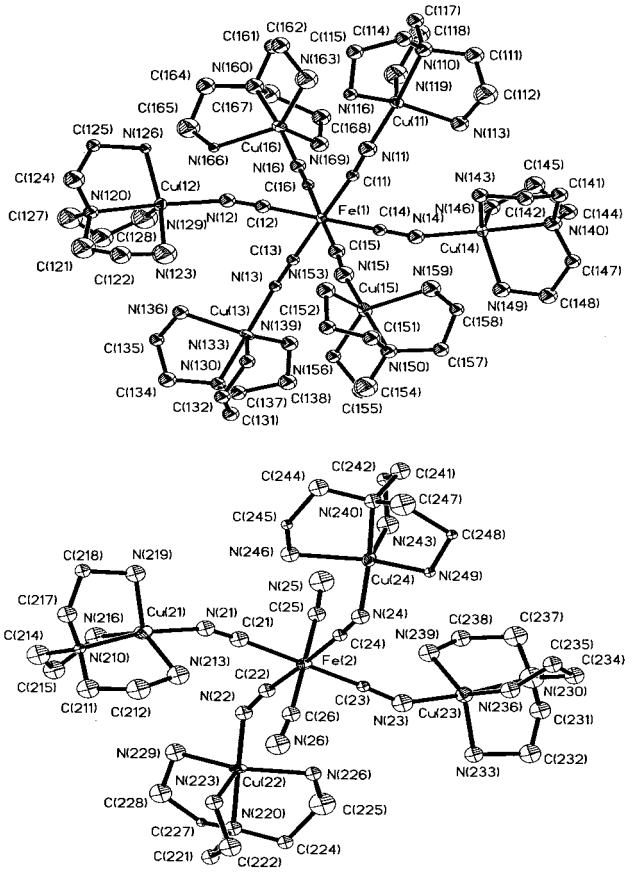

Figure 6. ORTEP diagrams of the: (a) heptanuclear cation, $[\{Cu(tren)CN\}_6Fe]^{8+}$, and (b) pentanuclear cation, $[\{Cu(tren)CN\}_4Fe(CN)_2]^{4+}$ of **4**, showing the atom labeling scheme and 50% thermal vibrational ellipsoids. Hydrogen atoms have been omitted for clarity.

$[Fe(CN)_6]^{4-}$, forcing the two terminal cyanides to adopt a trans orientation (Figure 6(b)). The charge on the cations is balanced by four $[Fe(CN)_6]^{3-}$ counteranions. DMSO (6) and water (21) molecules are also incorporated into the structure. Selected bond lengths and distances for the various components of **4** are listed in Tables 2 −4.

Hydrogen bonding interactions involving all solvent molecules, cations, and anions in **4** generate an extremely complex 3D network. Only three of the twenty-one water molecules make less than three H-bonding contacts each, and each of the six DMSO molecules makes at least one such contact. Twelve amine nitrogens on the heptanuclear complex and eight on the pentanuclear complex (as well as the two nonbridging and even one bridging cyano nitrogen) are involved in hydrogen bonds. Five of the nitrogens in the $[Fe(CN)_6]^{3-}$ anions centered on Fe(3) and Fe(6) are involved in hydrogen bonds, while three nitrogens participate in each of the Fe(4) and Fe(5) anions. The metal-containing moieties make no direct H-bonding interactions to each other, but rather are connected to each other via the solvent network.

The geometry of the iron centers within the heptanuclear and pentanuclear cores, and in the ferricyanide counteranions, matches that described for **1** and **3** showing little deviation from octahedral. Minor distortion of the ferrocyanide cores is reflected in the quasi-linear Fe−C−N angles, which are in the range of 171−179° for the heptanuclear cation and 167−177° for the pentanuclear cation. Greater variations in these angles are seen for the ferricyanide counteranions (162−179°) than for the heptanuclear cations in **1**, **3** and **4**, the pentanuclear cation in **4**, and values reported in the literature.[27,28,41,43,44,46−48,52] The Fe−C bond distances in the cations in **4** (1.84(2)−1.99(2) Å) show greater variation than in **1** and **3**, but are in agreement with those found in other Fe^{II} and Fe^{III}−C−N−Cu^{II} assemblies.[27,28,41,43−49] The Fe−C distances in the ferricyanide counteranions in **4** (1.83(2)−2.05(2) Å) span a wider range than those in **3** (1.89(2)−1.962(18) Å). The Fe···Cu separations (4.97 Å (average)) for the heptanuclear cation are similar to those in **1** and **3** and literature values.[46−49] On the other hand, shorter Fe···Cu distances are found in the pentanuclear cation (4.753−4.887 Å, average 4.82 Å) than in the heptanuclear cations of **1**, **3**, and **4**. This reduction in distance is due to the more acute Cu−N−C(cyano) angle subtended by the Fe−C−N−Cu bridging assembly.

The geometry of the Cu^{II} centers in both the heptanuclear and pentanuclear cations are generally in good agreement with those in **1** and **3**. However, the τ values[50] (0.45−0.84 for the heptanuclear cation and 0.57−0.73 for the pentanuclear cation) indicate greater distortion from ideal TBP than found in **3**. Despite these variations from ideal geometry, the $(R_3N)N-Cu-N(C-N)$ bond angles in all of the Cu^{II} moieties are almost linear (168.6(7)−179.1(7)°). As in **1** and **3**, the five-membered chelate rings gives rise to acute $H_2N-Cu-N$(amine) angles and out-

Table 2. Selected Bond Distances (Å) and Angles (Deg) for the Heptanuclear Cation, $[\{Cu(tren)CN\}_6Fe]^{8+}$, in **4**

Bond Distances			
Fe(1)−C(11)	1.93(3)	Cu(13)−N(133)	2.07(2)
Fe(1)−C(12)	1.93(3)	Cu(13)−N(136)	2.11(2)
Fe(1)−C(13)	1.93(2)	Cu(13)−N(139)	2.02(2)
Fe(1)−C(14)	1.91(2)	Cu(14)−N(14)	1.95(2)
Fe(1)−C(15)	1.84(2)	Cu(14)−N(140)	2.07(2)
Fe(1)−C(16)	1.97(2)	Cu(14)−N(143)	2.03(1)
Cu(11)−N(11)	1.94(2)	Cu(14)−N(146)	2.14(1)
Cu(11)−N(110)	2.07(2)	Cu(14)−N(149)	2.13(2)
Cu(11)−N(113)	2.04(2)	Cu(15)−N(15)	1.92(2)
Cu(11)−N(116)	2.14(2)	Cu(15)−N(150)	2.06(2)
Cu(11)−N(119)	2.07(2)	Cu(15)−N(153)	2.13(2)
Cu(12)−N(12)	1.96(2)	Cu(15)−N(156)	2.07(2)
Cu(12)−N(120)	2.04(2)	Cu(15)−N(159)	2.06(2)
Cu(12)−N(123)	2.03(1)	Cu(16)−N(16)	1.95(2)
Cu(12)−N(126)	2.03(1)	Cu(16)−N(160)	2.08(2)
Cu(12)−N(129)	2.19(2)	Cu(16)−N(163)	2.03(2)
Cu(13)−N(13)	2.00(2)	Cu(16)−N(166)	2.03(2)
Cu(13)−N(130)	2.03(2)	Cu(16)−N(169)	2.16(2)
Fe(1)···Cu(11)	5.032	Fe(1)···Cu(14)	4.894
Fe(1)···Cu(12)	4.889	Fe(1)···Cu(15)	4.983
Fe(1)···Cu(13)	5.030	Fe(1)···Cu(16)	4.985

Bond Angles			
Fe(1)−C(11)−N(11)	172.6(2)	Cu(14)−N(14)−C(14)	150.4(2)
Fe(1)−C(12)−N(12)	175(2)	Cu(15)−N(15)−C(15)	172.2(2)
Fe(1)−C(13)−N(13)	170.8(2)	Cu(16)−N(16)−C(16)	174.6(2)
Fe(1)−C(14)−N(15)	179(2)	N(11)−Cu(11)−N(110)	174.1(8)
Fe(1)−C(15)−N(15)	176(2)	N(11)−Cu(11)−N(113)	99.5(8)
Fe(1)−C(16)−N(16)	174.9(2)	N(11)−Cu(11)−N(116)	95.7(8)
C(11)−Fe(1)−C(12)	94.3(9)	N(11)−Cu(11)−N(119)	94.9(9)
C(11)−Fe(1)−C(13)	174.4(1)	N(110)−Cu(11)−N(113)	85.2(7)
C(11)−Fe(1)−C(14)	85.7(9)	N(110)−Cu(11)−N(116)	85.3(6)
C(11)−Fe(1)−C(15)	94.0(9)	N(110)−Cu(11)−N(119)	80.0(8)
C(11)−Fe(1)−C(16)	86.9(8)	N(113)−Cu(11)−N(116)	116.0(8)
C(12)−Fe(1)−C(13)	89.1(9)	N(113)−Cu(11)−N(119)	112.3(9)
C(12)−Fe(1)−C(14)	179.1(1)	N(116)−Cu(11)−N(119)	127.7(8)
C(12)−Fe(1)−C(15)	92.7(10)	N(12)−Cu(12)−N(120)	170.8(7)
C(12)−Fe(1)−C(16)	90.0(9)	N(12)−Cu(12)−N(123)	93.8(7)
C(13)−Fe(1)−C(14)	90.9(9)	N(12)−Cu(12)−N(126)	98.7(7)
C(13)−Fe(1)−C(15)	90.4(9)	N(12)−Cu(12)−N(129)	96.5(7)
C(13)−Fe(1)−C(16)	88.6(8)	N(120)−Cu(12)−N(123)	88.2(6)
C(14)−Fe(1)−C(15)	88.2(1)	N(120)−Cu(12)−N(126)	84.8(6)
C(14)−Fe(1)−C(16)	89.1(9)	N(120)−Cu(12)−N(129)	74.4(6)
C(15)−Fe(1)−C(16)	177.0(1)	N(123)−Cu(12)−N(126)	143.7(6)
Cu(11)−N(11)−C(11)	169.8(2)	N(123)−Cu(12)−N(129)	109.7(6)
Cu(12)−N(12)−C(12)	160(2)	N(126)−Cu(12)−N(129)	102.5(7)
Cu(13)−N(13)−C(13)	176.8(2)		

Table 3. Selected Bond Distances (Å) and Angles (Deg) for the Pentanuclear Cation, $[\{Cu(tren)CN\}_4Fe(CN)_2]^{4+}$, in **4**

Bond Distances			
Fe(2)−C(21)	1.99(2)	Cu(22)−N(226)	1.99(2)
Fe(2)−C(22)	1.90(2)	Cu(22)−N(229)	2.06(2)
Fe(2)−C(23)	1.85(2)	Cu(23)−N(23)	1.99(2)
Fe(2)−C(24)	1.88(2)	Cu(23)−N(230)	2.09(2)
Fe(2)−C(25)	1.93(2)	Cu(23)−N(233)	2.16(2)
Fe(2)−C(26)	1.89(2)	Cu(23)−N(236)	2.02(2)
Cu(21)−N(21)	1.93(2)	Cu(23)−N(239)	2.04(2)
Cu(21)−N(210)	2.06(2)	Cu(24)−N(24)	1.97(2)
Cu(21)−N(213)	2.08(2)	Cu(24)−N(240)	2.04(2)
Cu(21)−N(216)	2.07(2)	Cu(24)−N(243)	2.14(2)
Cu(21)−N(219)	2.13(2)	Cu(24)−N(246)	2.10(2)
Cu(22)−N(22)	1.96(2)	Cu(24)−N(249)	2.01(2)
Cu(22)−N(220)	2.07(2)	Fe(1)···Cu(22)	4.753
Cu(22)−N(223)	2.18(2)	Fe(1)···Cu(23)	4.861
Fe(1)···Cu(21)	4.887	Fe(1)···Cu(24)	4.777
Bond Angles			
Fe(2)−C(21)−N(21)	170(2)	Cu(23)−N(23)−C(23)	144.4(17)
Fe(2)−C(22)−N(22)	167(2)	Cu(24)−N(24)−C(24)	142(2)
Fe(2)−C(23)−N(23)	175.9(17)	N(21)−Cu(21)−N(210)	168.6(7)
Fe(2)−C(24)−N(25)	177(2)	N(21)−Cu(21)−N(213)	89.7(8)
Fe(2)−C(25)−N(25)	172(2)	N(21)−Cu(21)−N(216)	94.7(8)
Fe(2)−C(26)−N(26)	173(2)	N(21)−Cu(21)−N(219)	106.7(8)
C(21)−Fe(2)−C(22)	90.7(9)	N(210)−Cu(21)−N(213)	82.1(8)
C(21)−Fe(2)−C(23)	177.8(11)	N(210)−Cu(21)−N(216)	85.5(8)
C(21)−Fe(2)−C(24)	88.1(9)	N(210)−Cu(21)−N(219)	83.5(7)
C(21)−Fe(2)−C(25)	91.3(10)	N(213)−Cu(21)−N(216)	134.6(9)
C(21)−Fe(2)−C(26)	89.6(10)	N(213)−Cu(21)−N(219)	108.2(8)
C(22)−Fe(2)−C(23)	87.8(9)	N(216)−Cu(21)−N(219)	113.5(9)
C(22)−Fe(2)−C(24)	177.3(13)	N(22)−Cu(22)−N(220)	178.1(7)
C(22)−Fe(2)−C(25)	92.7(10)	N(22)−Cu(22)−N(223)	94.8(6)
C(22)−Fe(2)−C(26)	85.1(10)	N(22)−Cu(22)−N(226)	94.2(7)
C(23)−Fe(2)−C(24)	93.3(9)	N(22)−Cu(22)−N(229)	95.4(7)
C(23)−Fe(2)−C(25)	87.2(9)	N(220)−Cu(22)−N(223)	83.7(7)
C(23)−Fe(2)−C(26)	91.8(9)	N(220)−Cu(22)−N(226)	85.4(7)
C(24)−Fe(2)−C(25)	84.9(9)	N(220)−Cu(22)−N(229)	86.2(7)
C(24)−Fe(2)−C(26)	97.3(10)	N(223)−Cu(22)−N(226)	112.9(7)
C(25)−Fe(2)−C(26)	177.6(12)	N(223)−Cu(22)−N(229)	110.6(8)
Cu(21)−N(21)−C(21)	158(2)	N(226)−Cu(22)−N(229)	134.3(7)
Cu(22)−N(22)−C(22)	149(2)		

Table 4. Selected Bond Distances (Å) and Angles (Deg) for the Hexacyanoferrate(III) Anions in **4**

Bond Distances			
Fe(3)−C(31)	1.93(2)	Fe(5)−C(51)	1.92(2)
Fe(3)−C(32)	1.96(3)	Fe(5)−C(52)	1.90(2)
Fe(3)−C(33)	1.83(2)	Fe(5)−C(53)	1.90(2)
Fe(3)−C(34)	1.96(2)	Fe(5)−C(54)	1.95(2)
Fe(3)−C(35)	1.91(2)	Fe(5)−C(55)	1.98(2)
Fe(3)−C(36)	1.97(2)	Fe(5)−C(56)	1.98(2)
Fe(4)−C(41)	1.99(2)	Fe(6)−C(61)	2.05(2)
Fe(4)−C(42)	1.91(2)	Fe(6)−C(62)	1.93(2)
Fe(4)−C(43)	1.91(2)	Fe(6)−C(63)	1.97(2)
Fe(4)−C(44)	2.00(2)	Fe(6)−C(64)	1.96(2)
Fe(4)−C(45)	1.92(2)	Fe(6)−C(65)	1.92(3)
Fe(4)−C(46)	1.84(2)	Fe(6)−C(66)	1.98(2)
Bond Angles			
C−Fe(3)−C(cis)	86.7(8)−94.0(9)	C−Fe(5)−C(cis)	86.0(8)−94.0(8)
C−Fe(3)−C(trans)	176(1)−177.8(9)	C−Fe(5)−C(trans)	174.6(9)−178.6(7)
C−Fe(4)−C(cis)	85.9(9)−95.4(9)	C−Fe(6)−C(cis)	85.0(9)−94.1(9)
C−Fe(4)−C(trans)	176(1)−177.2(8)	C−Fe(6)−C(trans)	176(1)−178.4(9)
Fe−C−N	162(2)−179(2)		

of-plane displacements of the Cu^{II} centers toward the axial cyano ligands of ca. 0.22 Å.

The Cu−C−N angles in the pentanuclear cations (142−158°) show greater deviation from linearity than in the heptanuclear cation (150−177°). This could be due to steric interactions between the adjacent $[Cu(tren)]^{2+}$ moieties and/or to electrostatic interactions between the ferricyanide counteranions and water molecules associated with the complex. The trinuclear complex from which **4** is derived, $[\{Cu(tren)(CN)\}_2Fe(CN)_4]\cdot 12H_2O$, which has an Fe^{II} center bridging two $[Cu(tren)]^{2+}$ units, has a

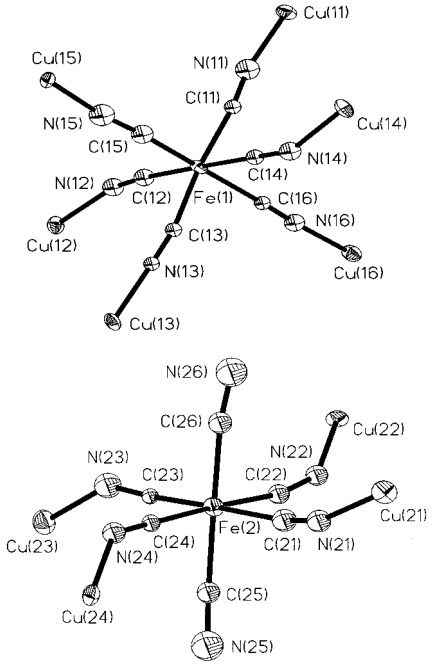

Figure 7. ORTEP plots of the backbones of the heptanuclear (a) and pentanuclear (b) components of **4** highlighting the bend in the Fe−C−N−Cu bridging units.

Table 5. UV−visible Spectral Data for Complexes **1**−**4**

	λ_{max}, nm (ϵ_{max}, $M^{-1}\,cm^{-1}$)	
	solid	solution
1	499, 665 sh, 855	**H_2O:** 515 (1200), 675 sh (817), 843 (1370)
2	458, 652 sh, 819	**H_2O:** 488 (986), 678 sh (704), 835 (879)
3	434, 492 sh, 670 sh, 821	**DMSO:** 423 (3000), 495 sh (1240) 668 sh (854), 822 (1020)

3D H-bonded network involving the water molecules.[46,49] It exhibits Cu−N−C(cyano) angles (144°) matching those in the pentanuclear cation, but they are 23° lower than the values found for the heptanuclear cation. Steric interactions between adjacent $[Cu(tren)]^{2+}$ units may force a quasi-linear arrangement of the Fe−C−N−Cu bridges in the heptanuclear cation (Figure 7(a)). The greater flexibility of the Fe−C−N−Cu bridge enables more acute angles to be subtended in pentanuclear cation, as highlighted in Figure 7(b).

Electronic Spectra. The solution electronic spectra (see Table 5) exhibit a band at 843 nm (1370 $M^{-1}cm^{-1}$) for **1**, 835 nm (879 $M^{-1}cm^{-1}$) for **2**, and 822 nm (1080 $M^{-1}cm^{-1}$) for **3** assignable to a d−d transition (d_{xy}, $d_{x^2-y^2} \rightarrow d_{z^2}$) of Cu^{II} moieties in TBP geometry. In each case, a high energy shoulder is observed at ca. 680 nm which is typical of Cu^{II} complexes with TBP geometry.[53,54] However, it should be recognized that these less intense shoulders can also arise from d−d transitions in copper(II) complexes with square pyramidal (SP) geometries.[55−57] The solid-state reflectance spectra of **1**−**3** show good correspondence to the solution spectra in the 600−900 nm region, indicating little stereochemical change on dissolution. The high energy shoulders have shifted to slightly lower λ (665 nm for

(55) Spiccia, L.; McLachlan, G. A.; Fallon, G. D.; Martin, R. L. *Inorg. Chem.* **1995**, *34*, 254.
(56) Haidar, R.; Ipek, M.; DasGupta, B.; Yousaf, M.; Zompa, L. *Inorg. Chem.* **1997**, *36*, 3125.
(57) Chaudhuri, P.; Oder, K.; Wieghardt, K.; Nuber, B.; Weiss, J. *Inorg. Chem.* **1986**, *25*, 2818.

1, 652 nm for **2**, and 670 nm for **3**) and are slightly more prominent than in the solution spectra. Again, the spectra are consistent with Cu^{II} complexes displaying distorted TBP geometry[54] in keeping with the solid-state structures. The greater prominence of these shoulders, compared to the corresponding solution spectra, may indicate a higher degree of distortion of the Cu^{II} centers toward SP geometry in the solid state. [62]

The solution electronic spectra of **1**−**3** exhibit one further band at 515 nm (1200 $M^{-1}cm^{-1}$) for **1**, 488 nm (986 $M^{-1}cm^{-1}$) for **2**, and 494 nm (shoulder, 1240 $M^{-1}cm^{-1}$) for **3**, which are ascribed to a metal to metal ($Fe^{II} \rightarrow Cu^{II}$) charge-transfer transition (MMCT).[58−60] Suzuki et al. have reported that Fe^{II}−CN−Cu^{II} bridged complexes can exhibit MMCT bands in the 400−515 nm range[58] ascribable to a one electron "jump" from the t_{2g} orbital of low spin Fe^{II} to the $d_{x^2-y^2}$ orbital of the Cu^{II} ion. Thus, the location of the MMCT band will depend on the energy gap between the $d_{x^2-y^2}$ orbital of the Cu^{II} ion and the t_{2g} orbital of the Fe^{II} ion. Assuming that the t_{2g} orbital energies of Fe^{II} remain constant, the MMCT transition will be tuned by the $d_{x^2-y^2}$ orbital energy of the Cu^{II} ions. A more intense band, located at 423 nm (3000 $M^{-1}cm^{-1}$) in the spectrum of **3**, is assigned to a $T_{2g} \rightarrow L(CN^-)_g$ symmetry forbidden charge-transfer transition within the counteranions from its correspondence with the spectrum of ferricyanide.[61] In the 400−500 nm region, the solid-state spectrum of complex **3** is virtually identical to the solution spectrum. For **1** and **2**, there is a general broadening and minor bathochromic shift of the bands (3−30 nm), such that they have λ_{max} values of 499 and 458 nm, respectively.

Magnetic Properties. The room-temperature magnetic moment (μ_{eff}) for **2** is 4.43 μ_B, marginally higher than the spin-only value of 4.24 μ_B expected for a spin system comprised of one Fe^{II} ($S = 0$) and six Cu^{II} ions ($S = 1/2$), and the complex exhibits Curie-like behavior as the temperature is lowered viz., $\mu_{eff} = 4.38\ \mu_B$ at 4.5 K. Complex **3** exhibits a room temperature μ_{eff} value of 5.61 μ_B (higher than the spin-only value 5.20 μ_B calculated for a spin system comprised of one Fe^{II} ($S = 0$), six Cu^{II} ions ($S = 1/2$), and two ferricyanide ions ($S = 1/2$)). The measured magnetic moment reproduces the decrease in moment observed for $K_3[Fe(CN)_6]$ as the temperature is lowered.[62−64] Thus, the diamagnetic Fe^{II} center is unable to mediate magnetic interactions between the paramagnetic Cu^{II} ions in the heptanuclear clusters, as was the case for **1**.[31]

Conclusion. Encapulation of ferrocyanide by six copper(II) moieties has been achieved through the use of tripodally coordinating tetradentate ligands. The Cu^{II} centers adopt TBP geometries with one axial site occupied by a nitrogen atom from cyanide ligand bound to the ferrocyanide core. The ability of Cu^{II} to form five-coordinate geometries is critical to the generation of these discrete heteropolynuclear assemblies. The use of tris(2-aminoethyl)amine has led to novel H-bonding assemblies which involve the secondary amines on this ligand, solvent molecules, and nitrogen atoms on the ferricyanide counteranions. Cocrystallization of the fully encapsulated heptanuclear and partially encapsulated pentanuclear Fe^{II}−Cu^{II} cations within the same lattice, $[\{Cu(tren)CN\}_6Fe][\{Cu(tren)CN\}_4Fe(CN)_2][Fe(CN)_6]_4 \cdot 6DMSO \cdot 21H_2O$ **4** has resulted from attempts to recrystallize $[\{Cu(tren)\}_2Fe(CN)_6]ClO_4 \cdot 2H_2O$.

Experimental Section

Physical Measurements. Ultraviolet−visible spectra were recorded in the range 200−1500 nm on a Varian Cary 5G spectrophotometer on solid samples (diffuse reflectance) or solutions. Infrared spectra were recorded as KBr pellets on a Perkin-Elmer 1600 series FTIR spectrometer. Room-temperature magnetic moments were measured on a Faraday balance, consisting of a four-inch Newport electromagnet and Cahn RG electrobalance based on a design described elsewhere.[65] Variable temperature magnetic susceptibility measurements were carried out as described elsewhere.[32] Conductivity measurements were made on a Crison 522 conductimeter at room temperature with Pt black electrodes at a concentration of 10^{-3} M. Standard 0.020 M KCl solution was used as a calibrant. Electron microprobe measurements were made with a Joel JSM-1 scanning electron microscope through an NEC X-ray detector and pulse processing system connected to a Packard multichannel analyzer. Solid samples were mounted on an aluminum planchet and covered with a very thin film of carbon using a Balzer Union CED 010 carbon sputterer. Mössbauer spectra were obtained in the transmission mode using a $^{57}Co(Rh)$ γ-ray source. The isomer shifts were referenced against natural α-iron foil at room temperature. The samples were crushed and placed in an iron free polymer sample holder. Curve fitting was performed using a least squares procedure and employed Lorenztian line shapes.

Materials and Reagents. All materials were of reagent grade or better and were used without further purification. Tris(2-pyridylmethyl)-amine (tpa) was prepared by a modification of the method of Anderegg and Wenk.[66] The mononuclear metal Cu^{II} complexes of tren[67] and tpa[68] were prepared according to published methods. In some cases, the Cu^{II} complexes were generated in situ and used directly in the synthesis of heterometallic complexes. Distilled water was used throughout. Methanol, dimethyl sulfoxide, dimethylformamide, and acetonitrile were dried by standing over activated 4 Å molecular sieves overnight.

Caution! *Although no problems were encountered in this work, transition metal perchlorates are potentially explosive. Such complexes should be prepared and handled with due care.*

Preparations. $[\{(CN)Cu(tpa)\}_6Fe][ClO_4]_8 \cdot 3H_2O$ (1). A solution of $[Cu(tpa)(OH_2)][ClO_4]_2$ (0.96 g, 1.7 mmol) in water (20 mL) was stirred and adjusted to pH 7 using 0.5 M sodium hydroxide, and a solution of $K_3[Fe(CN)_6]$ (92 mg, 0.28 mmol) in water (8 mL) was added dropwise resulting in the immediate precipitation of a purple powder, which was collected by filtration, washed successively with cold water, ethanol, and ether, and then air dried (yield: 0.66 g, 74%). A portion of the purple powder was dissolved in hot water, filtered, and the filtrate left to evaporate at room temperature. This yielded small dark purple crystals of **1** suitable for X-ray structure determination.

Characterization: Elemental analysis Calcd for $C_{114}H_{114}N_{30}Cl_8O_{35}Cu_6Fe$: C, 43.0; H, 3.6; N, 13.2. Found: C, 42.9; H, 3.6; N, 13.2. Selected infrared bands (cm^{-1}): 2109 vs (CN), 1607 vs (py), 1574 m (py), 1483 s (py). Electron microprobe: Cu, Fe, Cl present. UV−visible spectrum [λ_{max}, nm (ϵ_{max}, $M^{-1}\ cm^{-1}$) in H_2O]: 515 (1200), 675 sh (817), 843 (1370). Magnetic moment: μ_{eff} (290 K) = 4.41 μ_B per molecule. Molar conductivity: (Λ_m in H_2O): 770 S cm^2 mol^{-1}.

$[\{Cu(tren)CN\}_6Fe][ClO_4]_8 \cdot 10H_2O$ (2). A solution of $Cu(ClO_4)_2 \cdot 6H_2O$ (2.23 g, 6.02 mmol) in water (15 mL) was added to a stirring solution of tren (0.88 g, 6.03 mmol) in water (15 mL), resulting in a royal blue solution of $[Cu(tren)(OH_2)][ClO_4]_2$. A solution of $K_3[Fe(CN)_6]$ (0.33 g, 1.00 mmol) in water (30 mL) was then added dropwise, resulting in an immediate color change from royal blue to emerald. Once the addition was complete, the solution was left to slowly evaporate, and a dark green crystalline product formed. This was collected by filtration, washed successively with ethanol and ether, and then air-dried to give green crystals of **2** (yield: 1.41 g, 58%).

(58) Suzuki, M.; Uehara, A. *Bull. Chem. Soc. Jpn.* **1984**, *57*, 3134.
(59) Ludi, A.; Güdel, H. U. *Struct. Bonding* **1973**, *14*, 1.
(60) Morpurgo, L.; Mavelli, I.; Calabrese, L.; Finazzi, A.; Rotilio, G. *Biochem. Biophys. Res. Comm.* **1976**, *70*, 607.
(61) Naiman, C. S. *J. Chem. Phys.* **1961**, *35*, 323.
(62) Figgis, B. N.; Gerloch, M.; Mason, R. *Proc. R. Soc. Ser. A*: **1969**, *309*, 119.
(63) Fritz, J. J.; Rao, R. V. G.; Seki, S. *J. Phys. Chem* **1958**, *62*, 703.
(64) Guha, B. C. *Proc. R. Soc. London Ser. A*: **1951**, *206*, 353.
(65) Hill, J. C. *Sci. Instrum.* **1968**, *1*, 52.
(66) Anderegg, G.; Wenk, K. *Helv. Chim. Acta* **1967**, *50*, 2330.
(67) Albertin, G.; Bordignon, E.; Orio, A. *Inorg. Chem.* **1975**, *14*, 1411.
(68) Karlin, K.; Jacobson, R. R.; Tyeklar, Z.; Zubieta, J. *Inorg. Chem.* **1991**, *30*, 2035.

Table 6. Crystal Data for **3** and **4**

crystal data	**3**	**4**
chem formula	$C_{54}H_{139.6}Cl_2Cu_6Fe_3N_{42}O_{23.8}$	$C_{108}H_{258}Cu_{10}Fe_6N_{76}O_{27}S_6$
fw	2378.17	4216.76
space group	$P2_1/c$ (No. 14)	$P\bar{1}$ (No. 1)
a, Å	14.8674(10)	14.8094(8)
b, Å	25.9587(10)	17.3901(7)
c, Å	27.5617(10)	21.1565(11)
α, deg		110.750(3)
β, deg	100.8300(10)	90.206(2)
γ, deg		112.754(3)
V, Å^3	10447.7(9)	4635.7(4)
Z	4	1
λ (Mo Kα, Å)	0.71073	0.71073
D_{calc}, g/cm^3	1.512	1.510
μ(Mo Kα), cm^{-1}	17.3	17.19
T, K	123	123
R1[a](observed data)	0.0997	0.0902
wR2[b](all data)	0.3297	0.2512

[a] $R1 = \sum||F_o| - |F_c||/\sum|F_o|$. [b] $wR2 = [\sum w(F_o^2 - F_c^2)^2/\sum w(F_o^2)^2]^{1/2}$

.

Characterization: Elemental analysis Calcd for $C_{42}H_{128}N_{30}Cl_8O_{42}Cu_6Fe$: C, 20.6; H, 5.3; N, 17.2 Found: C, 20.7; H, 4.8; N, 17.0. Selected infrared bands (ν_{CN}, cm^{-1}): 2106 s. Electron microprobe: Cu, Fe, Cl present. UV−visible spectrum: [λ_{max}, nm (ϵ_{max}, M^{-1} cm^{-1}) in H_2O]: 488 (986), 678 sh (704), 835 (879). Magnetic moment: μ_{eff} (290 K) = 4.43 μ_B per molecule.

[{Cu(tren)CN}$_6$Fe][ClO$_4$]$_2$[Fe(CN)$_6$]$_2$·15.8H$_2$O (3). A solution of [Cu(tren)(OH$_2$)][ClO$_4$]$_2$ was prepared in situ by addition of an aqueous solution (35 mL) of Cu(ClO$_4$)$_2$·6H$_2$O (0.74 g, 2.00 mmol) to a stirring aqueous solution of tren (0.29 g, 2.00 mmol). The resultant royal blue solution was stirred for another 10 min before an aqueous solution (30 mL) containing K$_3$[Fe(CN)$_6$] (0.33 g, 1.0 mmol) and an excess of $K_2S_2O_8$ (0.33 g, 1.20 mmol) was added dropwise. Upon addition, the solution immediately changed color from royal blue to emerald. Slow evaporation of this solution at room temperature yielded emerald colored needles of **3** (yield: 0.19 g, 26%) suitable for X-ray crystallographic studies. These were collected by filtration, washed with water, and then air-dried.

Characterization: Elemental analysis Calcd for $C_{54}H_{139.6}N_{42}O_{23.8}Cl_2Cu_6Fe_3$: C, 27.3; H, 5.9; N, 24.7. Found: C, 27.0; H, 5.9; N, 24.2. Selected infrared bands (ν_{CN}, cm^{-1}): 2148 s, 2101 vs. Electron microprobe: Cu, Fe, Cl present. UV−visible spectrum [λ_{max}, nm (ϵ_{max}, M^{-1} cm^{-1}) in DMSO]: 423 (3000), 494 sh (1240), 668 sh (854), 822 (1080). Magnetic moment: μ_{eff} (295 K) = 5.61 μ_B per molecule.

[{Cu(tren)CN}$_6$Fe][{Cu(tren)CN}$_4$Fe(CN)$_2$][Fe(CN)$_6$]$_4$·6DMSO. 21H$_2$O (4). Recrystallization of [{Cu(tren)CN}$_2$Fe(CN)$_4$]ClO$_4$·2H$_2$O, prepared as described elsewhere,[39] from DMSO gave a few crystals of **4** that were suitable for single-crystal X-ray analysis.

Characterization: Selected infrared bands (ν_{CN}, cm^{-1}): 2110 s, 2100 s, 2080 vs, 2042 s.

X-ray Crystallography. A green needle of **3**, of approximate dimensions of 0.125 × 0.125 × 0.3755 mm, and a brown plate of **4**, of approximate dimensions of 0.125 × 0.125 × 0.025 mm, were mounted on glass fibers and used in data collection on a Nonius Kappa CCD area detector diffractometer with graphite monochromated Mo Kα radiation. For **3**, the data were collected to a maximum 2θ value of 25.36° with 0.5° oscillations and 15 s exposures. For **4**, data were collected to maximum 2θ value 30.07° with 1° oscillations and 45 s exposures. The data were processed using Nonius software[69] and were corrected for Lorentz and polarization effects.

The structures were solved by direct methods in SHELXS-86[70] and refined by full-matrix least squares based on F^2 in SHELXL-97.[71] For **3**, only the metal, chlorine, and oxygen atoms were refined anisotropically due to insufficient data. Of the twenty water molecules located in the structure, ten were refined at full occupancy, four at 70% site occupancy, and six at half occupancy, giving a total of 15.8 water molecules per formula unit. No hydrogen atoms were assigned to these solvent molecules. All other hydrogen atoms were assigned on the basis of geometric considerations and treated according to the riding model during refinement with isotropic displacement corresponding to the heavy atoms they are linked to. In the case of **4**, only the metal atoms were refined anisotropically. Four of the six DMSO molecules were disordered such that two positions for the sulfur atoms were assigned, with 0.67:0.33 site occupancy ratios. No hydrogen atoms were assigned to these disordered DMSO molecules or to the water molecules. All other hydrogen atoms (including those on the ordered DMSO molecules) were assigned and treated as for **3**. Refinement of **4** in the centrosymmetric space group $P\bar{1}$ resulted in disorder of some of the tren ligands over two positions; refinement in the noncentrosymmetric $P1$ removed this disorder. Thus, the final refinement of this structure was performed in this later space group, even though the vast majority of the structure is centrosymmetric. Refinement in $P1$ also indicated the crystal to be a racemic twin (final refined Flack parameter was 0.45(3)). Weighting schemes were employed for both structures, with $\omega = [\sigma^2(F_0^2) + (0.1873\ P)^2 + 66.10\ P]^{-1}$ for **3** and $\omega = [\sigma^2(F_0^2) + (0.1154\ P)^2 + 6.0864\ P]^{-1}$ for **4**, where $P = \{(\mathrm{Max}(F_0^2) + 2\ F_c^2)/3\}$. Crystal data are summarized in Table 6.

Acknowledgment. This work was supported by the Australian Research Council. R.J.P. was the recipient of a Monash Graduate Scholarship. We thank Dr B. Moubaraki and Professor K.S. Murray for performing magnetic susceptibility measurements.

Supporting Information Available: Two X-ray crystallographic files in CIF format. This material is available free of charge via the Internet at http://pubs.acs.org.

IC001452F

(69) (a) Hooft, R. *COLLECT Software*; Nonius BV, Delft: The Netherlands, 1998. (b) Otwinowski, Z.; Minor, W. In *Methods in Enzymology*, Carter, C. W., Sweet, R. M., Eds.; Academic Press: New York, 1996.

(70) Sheldrick, G. M. *SHELXS-86: Program for the solution of crystal structures*; University of Göttingen: Göttingen, Germany, 1986.

(71) Sheldrick, G. M. *SHELXL-97: Program for the refinement of crystal structures*; University of Göttingen: Göttingen, Germany, 1997.